Electronic Supplementary Information for the article

Kinetics of ^{1}H-^{13}C multiple-contact cross-polarization as a powerful tool to determine the structure and dynamics of complex materials : application to graphene oxide

Jésus Raya [a]*, Alberto Bianco [b] and Jérôme Hirschinger [a]*

[a]Institut de Chimie, UMR 7177 CNRS, Université de Strasbourg, Strasbourg, France
[b]University of Strasbourg, CNRS, Immunology, Immunopathology and Therapeutic Chemistry, UPR 3572, 67000 Strasbourg, France

*Corresponding authors :

hirschinger@unistra.fr

jraya@unistra.fr

Contents

This file contains the analysis of the ^{1}H MAS NMR spectrum (Section 1), T_1 and $T_{1\rho}$ relaxation data (Sections 2 and 3), MC-CP data (Section 4) of GO and simulations of static and MAS spectra (Section 5).

1. ^{1}H MAS NMR spectrum

The ^{1}H free induction decay following a single radiofrequency pulse is unfortunately perturbed by the backround signal of our CPMAS probe. This problem was overcome by applying the well-known two-pulse Hahn-echo sequence $\pi/2 - \tau - \pi -$ echo (1) (2). In order to optimize the refocusing of the magnetization the spin echo was synchronized with a rotational echo (3), *i.e.*, the delay τ between the pulses was fixed to an integer multiple of the rotor period $T_r = 1/\nu_r$. Whereas the resulting spectrum of GO at $\nu_r = 18$ kHz is still

significantly distorted by the wide probe signal for $\tau = T_r = 55.55$ μs (data not shown) the MAS synchronized spin-echo technique gives a rather poorly resolved but quantifiable signal with an overall linewidth of ~4.5 kHz surrounded by first-order spinning sidebands of low intensity when τ is increased to $6T_r = 333.33$ μs (Fig. S1). The subspectrum of each proton species may then be simulated by a set of spinning side bands (ssb's) separated by ν_r around an isotropic peak, each ssb being described by a Lorentzo-Gaussian line shape of full-width at half-height (FWHH) $\Delta\nu$. Since the anisotropy information is contained in the ssb intensities MAS allows separation of resonances with overlapping static line shapes. The ^{1}H MAS NMR spectrum was fitted using the solid line shape analysis (SOLA) package as implemented in the BRUKER™ TopSpin 4.0.8 software. Although the isotropic lines overlap this peak fitting procedure permits to distinguish three resonances at 3.0, 5.0 and 6.3 ppm representing 30%, 4% and 66% of the total signal, respectively (Fig. S1). Indeed, the presence of the rather sharp peak at 5.0 ppm ($\Delta\nu = 0.7$ kHz) and the wider resonance at 6.3 ppm ($\Delta\nu = 3.8$ kHz) is clearly demonstrated by inspection of their first-order ssb's (Fig. S1). Furthermore, the existence of the signal at 3.0 ppm appearing only as a shoulder in the spectrum of Fig. S1 is confirmed by the heterogeneous character of T_1 relaxation (see below). The interaction anisotropy of the minor peak at 5.0 ppm is readily observed to be much larger than the one of the major line at 6.3 ppm (Fig. S1). This is in agreement with previous assignments of peaks at 6.4 and 5.4 ppm to mobile water and strongly bound water, respectively (4). On the other hand, the ssb intensities for the signal at 3.0 ppm ($\Delta\nu = 4.7$ kHz) are found to be negligible. This shows that ν_r largely exceeds the anisotropic part of any nuclear spin interaction for this particular ^{1}H signal.

2. T_1 relaxation data

Using the line deconvolution of Fig. S1, it was possible to extract the magnetization recovery of the different ^{1}H chemical shifts. Fig. S2 displays the T_1^H inversion-recovery (IR) relaxation curves at 3.0, 5.0 and 6.3 ppm. The relaxation is, within experimental accuracy, exponential for the three resonances. The resulting T_1^H relaxation times (weight%) corresponding to the

sites at 3.0, 5.0 and 6.3 ppm are 48 ms (24%), 13 ms (2%) and 4.6 ms (74%), respectively. The ^{1}H magnetizations at 5.0 and 6.3 ppm then are expected to fully return to their equilibrium values in B_0 during the mixing time $\tau_M = 50$ ms of the MC-CP sequence (τ_M is longer than 3 times the spin-lattice relaxation time). On the other hand, the magnetization at 3.0 ppm must be partially saturated ($T_1^H \approx \tau_M$). Fortunately, 2D ^{1}H-^{13}C HETCOR spectra of GO demonstrate that only protons whose chemical shifts are between 4.5 and 7.5 ppm generate significant cross-peaks with the carbons (5). In other words, the signal at 3.0 ppm is irrelevant for the analysis of the MC-CP data since the ^{13}C spins are not efficiently polarized by these protons. This fits well with the fact that the signal at 3.0 ppm having no ssb's (Fig. S1) may be assigned to a third kind of mobile water molecules.

The ^{13}C IR data for the C-OH peak at (70 ppm) have been successfully fitted to a sum of two exponentials with time constants $T_{1S}^C = 0.2$ s and $T_{1L}^C = 6$ s (Fig. S3). Disregarding the irrelevant ^{1}H resonance at 3.0 ppm, this result clearly demonstrates that T_1^C is longer than T_1^H by at least an order of magnitude ($T_1^H < 0.01$ s).

3. $T_{1\rho}$ relaxation data

Extraction of relaxation data for individual resonances as done for the T_1^H measurements (Fig. S2) was also attempted in the case of the direct $T_{1\rho}^H$ relaxation experiments. Unfortunately, this analysis was unsuccessful due to the presence of lineshape distortions even when using a long delay τ between the end of the spin-lock and the application of the additional refocusing pulse. Hence, the integrated intensity of the whole ^{1}H MAS NMR spectrum was fitted instead. The $T_{1\rho}^H$ relaxation decays fit well to two-exponential curves irrespective of the value of the delay τ (Fig. S4). Moreover, the short ($T_{1\rho S}^H$) and long ($T_{1\rho L}^H$) relaxation times are determined with a good accuracy since they differ by an order of magnitude. The variation of the component intensities with the spin-echo delay τ is easily explained by the effect of transverse relaxation. Indeed, $T_{1\rho S}^H$ and $T_{1\rho L}^H$ are expected to be respectively associated with short and long T_2^H relaxation components (6) (7). In principle,

$T_{1\rho S}^{H}$ and $T_{1\rho L}^{H}$ should be essentially independent of τ. Although this is the case for the long component ($T_{1\rho L}^{H} \approx$ 2 ms) $T_{1\rho S}^{H}$ increases from 0.05 to 0.3 ms when increasing τ from 55.55 μs to 333.33 μs (Fig. S4). This result is readily attributed to a remaining contribution of the probe signal and/or the presence of an inhomogeneous distribution of correlation times (6) (7) as well as to the fact that the fast-relaxing component is almost completely determined by the intensity of the first point of the relaxation curve at $t_{SL} = 120$ μs when $\tau = 55.55$ μs (Fig. S4(a)). Indeed, 3 parameter fits of the $T_{1\rho}^{H}$ relaxation data with $T_{1\rho S}^{H}$ and $T_{1\rho L}^{H}$ fixed to 0.1 ms and 2 ms, respectively, results in an increase of the χ^2 merit function (8) by only a factor of ~3 when compared to the 5 parameter fits of Fig. S4. It may then be concluded that two main relaxation components with $T_{1\rho S}^{H} \sim$ 0.1 ms and $T_{1\rho L}^{H} \approx$ 2 ms are clearly observed in GO by direct $T_{1\rho}^{H}$ measurements although a precise determination of $T_{1\rho S}^{H}$ is impossible because this relaxation component decays very fast and is affected by the backround signal of the probe. Note finally that this problem cannot be solved by indirect $T_{1\rho}^{H}$ measurement through ^{13}C magnetization because of low polarization transfer efficiency at short contact times ($t_{CP} <$ 0.1 ms).

$T_{1\rho}$ relaxation is, within experimental accuracy, exponential for all ^{13}C resonances. $T_{1\rho}^{C}$ is determined to be 7.4 ms for the C-OH peak (Fig. S5). Similar results are obtained for the C-O-C ($T_{1\rho}^{C} =$ 9.2 ms) and C=C ($T_{1\rho}^{C} =$ 7.0 ms) resonances (data not shown). Note however that the presence of a longer $T_{1\rho}^{C}$ component cannot be excluded because the maximum spin-lock duration employed in the measurements was only 10 ms.

4. MC-CP data at 70 ppm

Two T_{IS}^{MC} components can be separated in the MC-CP experiments with $t_{CP}/n = 277.5$ μs at the C-OH resonance (Fig. S6). Indeed, the distribution of the residuals for a one and two-exponential fit clearly demonstrates the two-exponential nature of build-up curve ($T_{IS}^{MC(2)}/T_{IS}^{MC(1)} \approx$ 4). A separation into two components is outside experimental accuracy

for the MC-CP experiment at $t_{CP}/n = 555$ μs (*cf*. Fig. 8 in the main text) which is well fitted by an exponential curve with $T_{IS}^{MC} = 0.7$ ms (not shown).

5. Simulations of static and MAS NMR spectra

Simple analytical treatments to describe the spin dynamics in powders under the simultaneous action of local fields produced by either chemical-shift anisotropy or dipolar couplings, intermediate regime motions, and MAS have been presented in several articles (9) (10) (11) (12) (13) (14). The spectra of Fig. S7 calculated for a diffusive isotropic or anisotropic Gaussian-Markov process according to Ref. (12) reproduce the relevant features of the static and MAS ^{1}H spectra discussed in the main text. An interproton distance of 1.62 Å within the water molecule corresponds to a powder-averaged second moment $M_2 = 3.189\times10^{10}\ \mathrm{s}^{-2}$ ($1/\sqrt{M_2} = 5.6\ \mu\mathrm{s}$).

References

1 E. L. Hahn, *Phys. Rev*., 1950, **80**, 580-594.

2 M. Rance, R. A. Byrd, *J. Magn. Reson.*, 1983, **52**, 221-240.

3 E. T. Olejniczak, S. Vega, R. G. Griffin, *J. Chem. Phys.*, 1984, **81**, 4804-4817.

4 A. Lerf, H. He, M. Foster, J. Klinowski, *J. Phys. Chem. B*, 1998, **102**, 4477-4482.

5 I. A. Vacchi, C. Spinato, J. Raya, A. Bianco, C. Ménard-Moyon, *Nanoscale*, 2016, **8**, 13714-13721.

6 V. J. McBrierty, K. J. Packer, *Nuclear magnetic resonance in solid polymers.* Cambridge : Cambridge University Press, 1993.

7 K. Schmidt-Rohr, H. W. Spiess, *Multidimensional Solid-State NMR and Polymers.* London : Academic Press, 1994.

8 W. H. Press, B. P. Flannery, S. A. Teukolsky, W. T. Vetterling, *Numerical Recipes.* Cambridge : Cambridge University Press, 1986.

9 D. Suwelack, W. P. Rothwell, J. S. Waugh, J. Chem. Phys., 1980, **73**, 2559-2569.

10 S. Clough, K. W. Gray, Proc. Phys. Soc., 1962, **79**, 457-467.

11 D. Fenzke, B. C. Gerstein, H. Pfeifer, *J. Magn. Reson*., 1992, **98**, 469-474.

12 J. Hirschinger, *Concepts Magn. Reson. Part A*, 2006, **28**, 307-320.

13 E. R. deAzevedo, K. Saalwächter, O. Pascui, A. A. de Souza, T. J. Bonagamba, D. Reichert, *J. Chem. Phys.*, 2008, **128**, 104505.

14 J. Hirschinger, *Solid State Nucl. Magn. Reson.*, 2008, **34**, 210-223.

Fig. S1
Raya et al

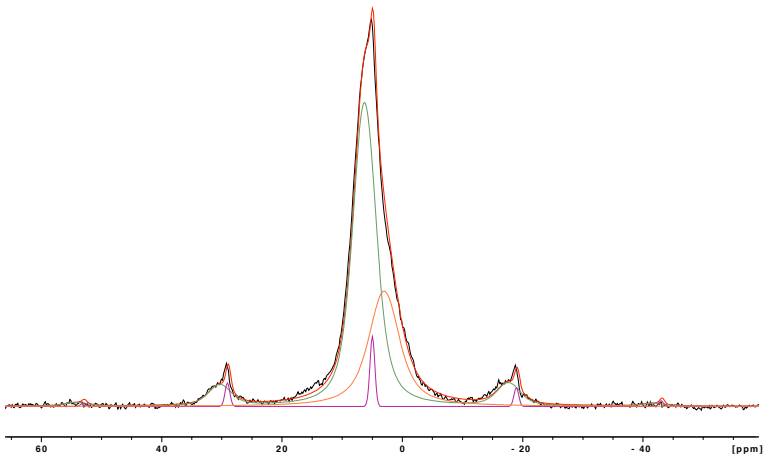

Figure S1 : Deconvolution of the MAS spin-echo ^{1}H NMR spectrum of GO (black line) at $\nu_r =$ 18 kHz ($\tau = 6T_r =$ 333.33 μs). The fitted spectrum (red line) is the weighted sum of the subspectra at 3.0 ppm (orange line), 5.0 ppm (purple line) and 6.3 ppm (green line).

Fig. S2
Raya et al

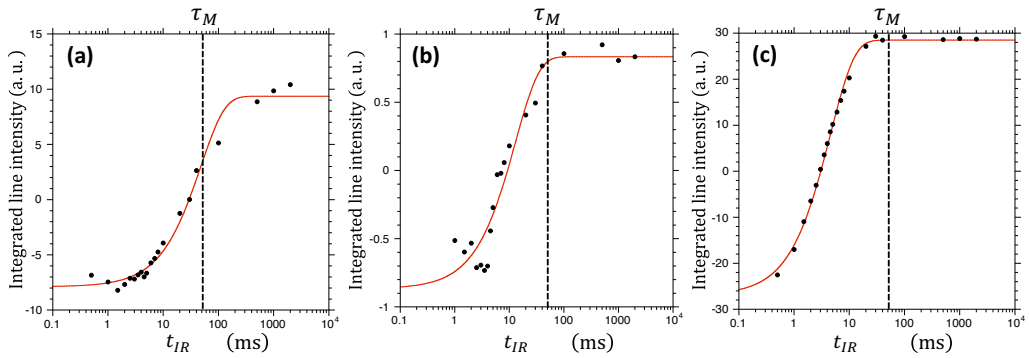

Figure S2 : ^{1}H spin-lattice relaxation in the laboratory frame by the inversion-recovery (IR) pulse sequence with spin-echo ($\tau = 6T_r = 333.33$ μs). The spin-lattice relaxation times (component weight%) obtained by exponential fitting (red line) of the deconvoluted IR data corresponding to the subspectra of Fig. S1 at (a) 3.0 ppm, (b) 5.0 ppm and (c) 6.3 ppm are $T_1^H = 48$ ms (24%), $T_1^H = 13$ ms (2%) and $T_1^H = 4.6$ ms (74%).

Fig. S3
Raya et al

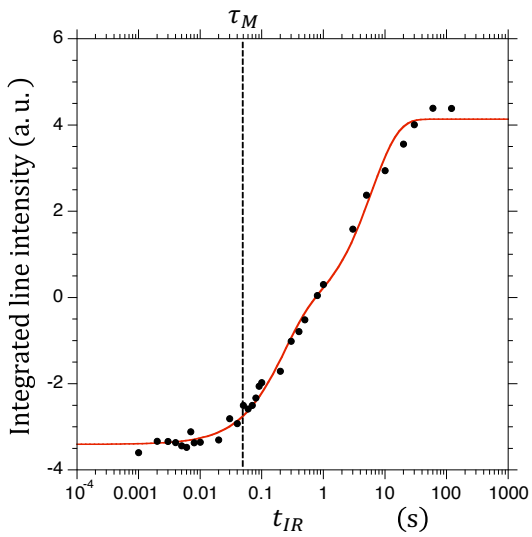

Figure S3 : ^{13}C spin-lattice relaxation in the laboratory frame by the IR pulse sequence with spin-echo ($\tau = T_r = 55.55$ µs) for the C-OH resonance (70 ppm). The two-exponential fit (red line) of the data gives the relaxation times (component weight%) $T_{1S}^C = 0.2$ s (39%) and $T_{1L}^C = 6$ s (61%).

Fig. S4
Raya et al

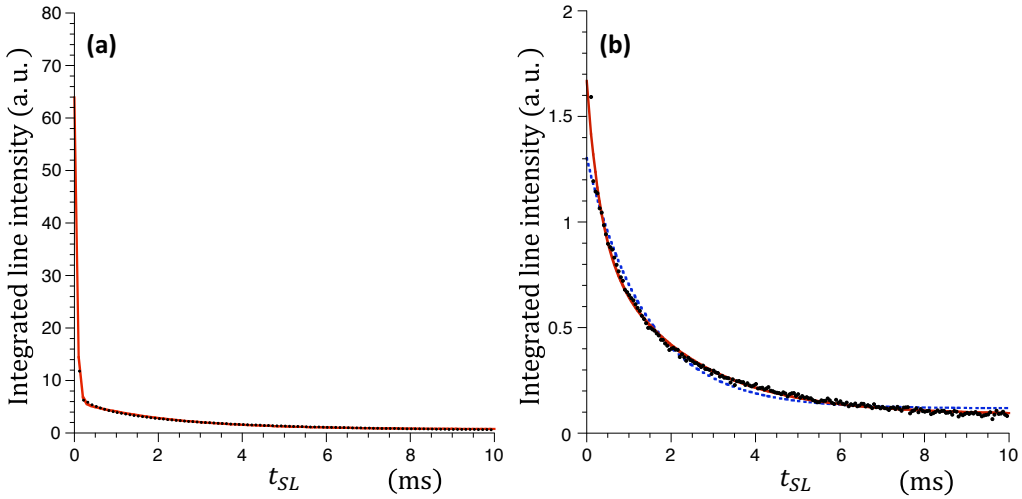

Figure S4 : ^{1}H spin-lattice relaxation in the rotating frame by the spin-lock (SL) pulse sequence including spin-echo with (a) $\tau = T_r = 55.55$ µs and (b) $\tau = 6T_r = 333.33$ µs. The two-exponential fit (red solid line) of the SL data gives the relaxation times (component weight%) : (a) $T_{1\rho S}^{H} = 53$ µs (91%) and $T_{1\rho L}^{H} = 2.2$ ms (9%) ; (b) $T_{1\rho S}^{H} = 0.3$ ms (46%) and $T_{1\rho L}^{H} = 2.1$ ms (54%). The exponential fit (blue dotted line) in (b) yielding $T_{1\rho}^{H} = 1.4$ ms clearly demonstrates the two-exponential nature of the relaxation decay.

Fig. S5
Raya et al

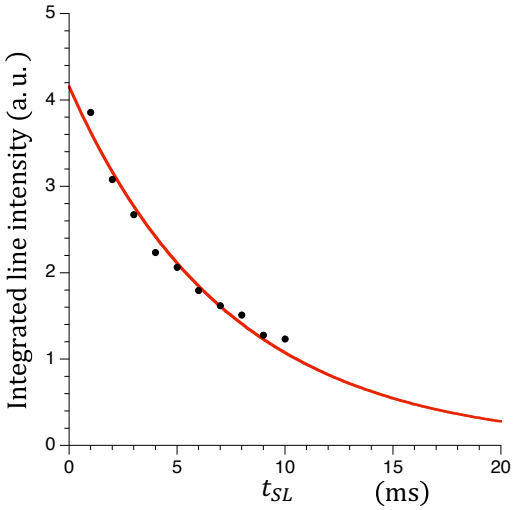

Figure S5 : ^{13}C spin-lattice relaxation in the rotating frame by SL pulse sequence with spin-echo ($\tau = T_r = 55.55$ μs) for the C-OH resonance (70 ppm). The exponential fit (red line) of the SL data gives the relaxation time $T_{1\rho}^{C}$ =7.4 ms.

Fig. S6
Raya et al

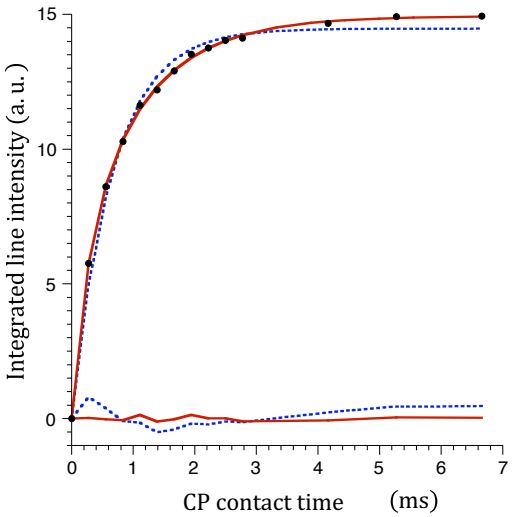

Figure S6 : Time dependence of the ^{13}C magnetization in the MC-CP experiment with $t_{CP}/n = 277.5$ µs for the C-OH resonance (70 ppm) of GO. The two-exponential fit (red solid line) of the MC-CP data gives the time constants (component weight%) $T_{IS}^{MC(1)} = 0.25$ ms (36%) ; $T_{IS}^{MC(2)} = 1.1$ ms (64%). The exponential fit (blue dotted line) of the MC-CP data yields T_{IS}^{MC} =0.66 ms. The distribution of the residuals for the one and two -exponential fit is reported at the bottom of the plot.

Fig. S7
Raya et al

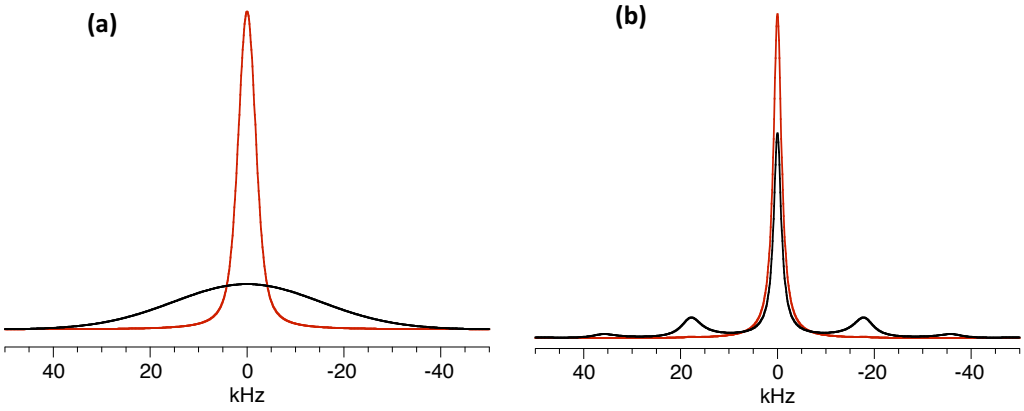

Figure S7 : (a) static and (b) MAS ($\nu_r = 18$ kHz) NMR spectra for isotropic *slow*-exchange narrowing due to spin diffusion (black line) and anisotropic *fast*-exchange narrowing due to molecular motion (red line) calculated for a diffusive Gaussian-Markov process according to Ref. (12). The parameters are $1/\sqrt{M_2} = 10$ μs and $\tau_B = 100$ μs for the rigid (slow-exchange) component lineshape ; $1/\sqrt{M_2^{LT}} = 5.6$ μs, $1/\sqrt{M_2^{HT}} = 120$ μs and $\tau_c = 0.2$ μs for the mobile (fast-exchange) component lineshape.